NATIONAL ADVISORY COMMITTEE FOR AERONAUTICS

TECHNICAL NOTE 4162

STUDY OF SOME BURNER CROSS-SECTION CHANGES THAT INCREASE SPACE-HEATING RATES

By Donald R. Boldman and Perry L. Blackshear, Jr.

Lewis Flight Propulsion Laboratory
Cleveland, Ohio

Washington
November 1957

NATIONAL ADVISORY COMMITTEE FOR AERONAUTICS

TECHNICAL NOTE 4162

STUDY OF SOME BURNER CROSS-SECTION CHANGES THAT INCREASE SPACE-HEATING RATES

By Donald R. Boldman and Perry L. Blackshear, Jr.

SUMMARY

Measurements of turbulent flame speeds and space-heating rates were made in a 1/2- by 2-inch glass-walled burner in which area blockage was introduced. Certain conclusions may be drawn. Blockage is more beneficial when introduced downstream of a flameholder than at the flameholder; that is, for equivalent pressure drops, heat-release rates of the former are about four times the latter. The shape of the blockage influences the gains in heat-release rate; symmetric obstructions that restrict the flow for a finite length are found to be more effective than abrupt restrictions. When a flameholder is placed within or immediately upstream of a convergent section, the flame is prone to blow out; however, for a divergent section blowout does not occur.

INTRODUCTION

Recent work (ref. 1) has shown that a flame anchored in a duct creates a velocity field that is moderately unstable under some important circumstances. Owing to this instability, incoming turbulence is amplified; hence, turbulent flame propagation is increased. Because the flow is only moderately unstable, turbulence due to this instability is not as great; hence, turbulent flame speed is not as high as it could be were steps taken to further excite this unstable velocity field. Two methods are suggested in reference 1: (1) supply the flow with the kind of disturbance the flow field could amplify, or (2) supply a change in combustor cross section that would permit the existing disturbance to be more rapidly amplified. In reference 1 the method examined consisted of introducing disturbances that the flow field could amplify. For example, a flame anchored in a duct propagated with a velocity twice the laminar velocity; when excited at a suitable frequency at the flameholder, the propagation velocity approached three times laminar. This result is related to the instability of the velocity profile that spontaneously arises when a flame is anchored in a duct of constant cross section.

When the cross-sectional area is altered downstream of the flameholder, the resulting pressure gradients acting on gases of differing densities cause new velocity profiles to arise. Most of the new profiles are more unstable than the spontaneous ones; consequently, the propagation velocity is higher. The introduction of changes in cross section is accompanied by additional pressure drop.

In the present investigation method (2) of promoting turbulent flame propagation is explored by adding blockage configurations downstream of a simple baffle flameholder in a two-dimensional combustor and observing the results.

The observations consist of measuring and comparing the combustion efficiencies, the ratio of turbulent to laminar flame speed V_T/V_L (symbols are given in appendix A), and the pressure drops for a number of configurations. The purpose is to find the effect of configuration shape on flame propagation and pressure drop. In the course of the work, a single configuration was found that gave an outstanding increase in V_T/V_L and, hence, in combustion efficiency, with a total-pressure loss that is not prohibitive. The distribution of the burning zone for this configuration was examined in detail and is described herein.

This and additional information serve as a basis for giving a qualitative description of the beneficial processes that take place in the flow of a flame through a restriction.

APPARATUS

General

Flow metering. - Air and propane flows were metered by rotameters and were thoroughly mixed before they were introduced into the combustor.

Combustor. - The basic combustor consisted of a 1/2- by 2-inch test section 12 inches long with glass side walls (fig. 1); it is described more fully in reference 1.

The basic flameholder, a 60° gutter 0.306 inch wide, spanned the 1/2-inch dimension. The gutter position could be varied axially.

Test Configurations

To the basic combustor were added various restrictions that altered the duct area. The restrictions were located downstream of the flameholder and were made of 0.050-inch brass and supported by screws in the upper and lower walls. Figure 2 contains sketches of the restrictions.

Symmetric series. - The series A to F in figure 2(a) (also shown in table I) illustrate configurations where the length of the throat was held constant as burner cross-sectional blockages were varied from $62\frac{1}{2}$ percent to 0 in $12\frac{1}{2}$-percent intervals. The configurations G to I (fig. 2(b)) comprised a constant $62\frac{1}{2}$-percent blockage with varying throat lengths; configuration A fits this sequence also. The wavy-wall contours of J and K (fig. 2(c)) provided $62\frac{1}{2}$- and $37\frac{1}{2}$-percent blockages, respectively. For the flameholder L (table I), blockages were varied from $12\frac{1}{2}$ percent to 75 percent in $12\frac{1}{2}$-percent intervals.

Asymmetric series. - The asymmetric configurations shown in figures 2(d) and (e) consist of airfoil-shaped blockage devices of various sizes and positions. The downstream surface of configuration M was shortened while maintaining a $37\frac{1}{2}$-percent blockage to give configurations N and O. The positions of two airfoils of different size were varied to give configurations P to S. All provide $62\frac{1}{2}$-percent projected area blockage. The wavy-wall configuration T also blocked $62\frac{1}{2}$ percent of the projected area.

Instrumentation

Photomultiplier. - A photomultiplier tube (fig. 3), supplied by a steady direct-current source, sensed light through successive 1/4- and 1/16-inch-wide apertures spaced 2 feet apart in a rectangular probe. A mask containing a 1/8- by 1/4-inch aperture adaptable to the front of the probe was available. Relative flame luminosity was obtained from a direct-current voltmeter connected to the photomultiplier tube.

Pressure measurement. - Plenum pressures were obtained from a U-tube water manometer. The height of the water column was measured to the nearest 1/32 inch.

PROCEDURE

Determination of Ratio of Turbulent to Laminar Flame Speed

In reference 2, using photomultiplier tubes, it was found that turbulent and laminar flames with identical fuel-air ratios and flow rates produce equal average light intensities. This fact was used in reference 1 as a basis of the assumption that photomultiplier tubes can be used to obtain average heat-release rates. This assumption was experimentally verified in the apparatus used herein.

The ratios of turbulent to laminar flame speed V_T/V_L can be defined as the ratios of the heat released per unit length to the heat that a pair of laminar flames parallel to the burner axis would release per unit length per unit time. These quantities were measured as described below.

The photomultiplier views a narrow strip of the burner section. Voltages from the photomultiplier tube must be obtained for a turbulent flame and again for a laminar flame while maintaining a constant fuel-air ratio. The flame-front half angle is measured in each case from a picture of the entire flame, and each voltage is multiplied by the cosine of the half angle. The ratio of the resulting product for the turbulent flame to that for the laminar flame is defined as V_T/V_L. For turbulent flames the cosine of the half angle can be assumed equal to unity so that the unit length of the flame fronts becomes the unit length of the combustor.

In this investigation values of laminar flame speed V_L were taken from reference 3. The voltage E_L for the photomultiplier probe used was determined in reference 1 for laminar flames of several fuel-air ratios. Figure 4 shows the variation of V_L and E_L with fuel-air ratios. Since photomultiplier tube output voltage is proportional to light intensity, V_T/V_L can be expressed as follows:

$$V_T/V_L = E_T/E_L$$

Determination of Volumetric Heat-Release Rate

Volumetric heat-release rates q were obtained on the basis of turbulent flame speed V_T and the following equation:

$$q = \frac{\text{Flame speed} \times \text{flame area} \times \text{heating value/unit vol.}}{\text{Volume of combustor viewed}}$$

$$= \frac{2gV_T\rho_a Qf\ 3600}{\text{Aperture height}}$$

where aperture height is in feet and determines the volume of combustor viewed. The large aperture was used to measure average q at each station along the burner. The mask containing the small aperture was used to limit the height of the slit and to permit scanning across the duct, thus providing volumetric heat-release rates at 1/8-inch increments normal to burner axis.

Determination of Pressure Drop

The ratio of the actual total-pressure drop across the combustion zone to that of the ideal one-dimensional case provided a basic comparison parameter. The equation for the pressure-drop parameter is derived in appendix B and can be written as

$$\frac{\Delta P}{\Delta P_{1D}} = \frac{\left(\frac{U_1}{U_0}\right)^2 - \frac{F^2(T_b/T_0)}{\left[1 - (1 - F)\frac{U_0}{U_1}\right]^2}}{\frac{T_b}{T_0} - 1}$$

Determination of Combustion Efficiency

Combustion efficiency, which is a direct function of turbulent flame speed, is given by the following expression:

$$\eta_c = \frac{\text{Average flame velocity} \times \text{flame area}}{\text{Total volume flow rate}}$$

$$= \frac{\text{Average } V_T \times 2 \times \text{length of flame}}{U_0 \times \text{Height of test section}}$$

In most of the runs, the combustor length was 9 inches. In those runs where it was not the values of V_T were extrapolated so that all the combustion efficiencies reported would be for the same combustor length.

RESULTS

A summary of the results obtained at 50 feet per second and a fuel-air ratio of 0.0456 is given in table I. The configurations tested are shown and the following information given: maximum blockage, maximum turbulent flame speed, combustion efficiency, pressure drop, and the pressure-drop parameter $\Delta P/\Delta P_{1D}$.

Effects of Fuel-Air Ratio and Velocity Variation

The effects of varying the fuel-air ratio and velocity can be seen in the plots of V_T/V_L against distance from the flameholder (fig. 5)

for the representative configurations A to F. Although the behavior of V_T/V_L downstream of the restriction varies from configuration to configuration, certain characteristics were noted. (1) On entering the restriction V_T/V_L is reduced in many cases. This reduction is less marked as U decreases or V_L increases. (2) In general, the higher the approach flow velocity, the higher V_T/V_L becomes. (3) In some instances V_T/V_L goes through a maximum and begins to decline downstream of the restriction. The maximum moves closer to the restriction as V_L is increased and U is decreased.

Effect of Restriction Shapes

It was suggested in reference 1 that wavy walls serve (1) to introduce transverse disturbances having wavelengths that the flow could amplify and (2) to increase the amplification rate by making the velocity profile more unstable.

According to reference 1, an asymmetric flow disturbance should increase flame speed more rapidly than a symmetric one. Inspection of table I shows that the symmetric series A to F gave V_T/V_L and η_c values that are superior to those found on the asymmetric series. It would appear then that of the two arguments for the wavy wall argument (2) is the more important. This matter will be discussed further in appendix C.

Effect of Flameholder Size Without Downstream Restriction

A series of tests were made on flameholders varying in width from 0.306 to 1.5 inches (configuration L). The results of these runs are shown in figures 6 and 7. In figure 6 V_T/V_L against distance along the duct is shown for two velocities.

Figure 7 shows a plot of $\Delta P/\Delta P_{1D}$ and peak values of V_T/V_L against flameholder blockage for a velocity of 50 feet per second. An increase in blockage by the flameholder causes an increase in the pressure-drop parameter, but does not affect the peak V_T/V_L values. In the series A to F an increase in blockage resulted in an increase in $\Delta P/\Delta P_{1D}$ as well as an increase in the peak V_T/V_L (fig. 5 and table I). The effect of these two different kinds of blockage are compared in figure 8, where the combustion efficiency is plotted as a function of the total-pressure-loss parameter $\Delta P/\Delta P_{1D}$.

It is apparent that for this range of variables downstream blockage is more beneficial.

Also shown for comparison is the series G to I as well as the airfoil shape R, again demonstrating that the effect of downstream blockage is influenced by shape.

Heat-Release Rates

Configuration A gives a relatively high efficiency without excessive ΔP. It is of interest to see how its space-heating rates compare with Longwell's (ref. 4). Figure 9 shows longitudinal and transverse plots of volume heating rates obtained by the method outlined in PROCEDURE. The maximum local value of 18.5×10^6 Btu per hour per cubic foot is about 1/5 the maximum value extrapolated from Longwell's results adjusted for fuel-air ratio, temperature, pressure, and fuel type (see ref. 4). It would appear, then, that though the volume heating rate is of the same order of magnitude, substantial gains can still be made.

Blockage is more beneficial when introduced downstream of a flameholder than at the flameholder as can be noted from figures 5 and 6. For equivalent pressure drops, heat-release rates downstream, as indicated by the turbulent flame speed, are about four times those at the flameholder.

Flame Blowout and Interruption by Restrictions

Figure 10 shows the trace of V_T/V_L against distance downstream from the inlet for the flameholder at different positions relative to the obstruction. If the flameholder is located where the cross-sectional area is increasing (i.e., $dA/dx > 0$) the V_T/V_L values climb rapidly downstream of the flameholder. When the flameholder is situated at or just upstream of the region where $dA/dx < 0$, the flame is blown off. This behavior occurred at every condition tested where downstream blockage was greater than 25 percent. In most cases the flame blowoff occurred with complete flame extinction. With the flameholder at some positions upstream of the restriction it was possible to cause the flame to blow off at the plane of the restriction leaving the recirculating zone just downstream of the flameholder and part of the propagating flame intact. When the flameholder was moved swiftly through the restriction, this attached zone would remain; if moved slowly, the zone would blow off. When the flameholder was moved 2 inches or more upstream of the restriction, the flame would once more propagate through.

An effort was made to see if the flame could be extinguished at the throat by increasing the restriction, or the velocity, or both, with the flameholder well upstream of the restriction. In every case where the flame failed to propagate through the restriction, the flame zone entering the restriction was on the order of the laminar flame thickness (ref. 5). For the most part, if the flame was well established upstream, it was impossible to extinguish the flame at the restriction by merely decreasing the open area. On the other hand, if the recirculation zone was brought near the restriction, the flame was quite easily cut off at the restriction. A photograph of such a flame is given in figure 11.

Flow Tracer Study

Because the downstream divergence angle was very large on most of the configurations, flow separation occurred when there was no flame present. When the flame was present, the contour of the flame made it appear that no separation occurred at the wall; qualitative considerations in appendix C suggest that reversal might be expected within the hot-gas zone rather than in the cold-gas boundary. To examine for the existance of flow reversal, a hot wire coated with sodium bicarbonate was moved about inside the combustor with configuration A in place. No reverse-flow region was found anywhere in the combustor except in the immediate wake of the flameholder, that is, the usual flameholder recirculation zone.

The length of the recirculating zone is strongly influenced by convergent and divergent walls; it increases if the walls diverge, decreases if the walls converge.

Shadow and Direct Photographs of the Flame

Figure 11 shows photographs of some of the flames studied. Figures 11(a) and (b) show the flame without contraction; figures 11(c) and (d) show the flame with configuration A in place. The shadowgraph, figure 11(d), shows evidence of very fine grained density variation downstream of the constriction, suggesting the presence of fine-scale turbulence. The direct photograph, figure 11(e), is at a slightly leaner condition than the others; the flame has failed to propagate through the restriction.

DISCUSSION

The data presented show that introducing additional blockage can either increase (downstream blockage) or slightly impair (flameholder blockage) combustion efficiency. The most encouraging ways of

introducing blockage are, of course, those in which the blockage is downstream of the flameholder. There are two main questions if this method is to be used: (1) When the area is reduced, how can flame interruption be avoided, and (2) when area is decreased and then increased, what is the fundamental mechanism that determines beneficial flame propagation stimuli? An adequate answer to these questions is beyond the scope of the present work. A qualitative answer might help to define the problem and is therefore included in appendix C.

The specific results of the considerations in appendix C are these: The flame will be quenched in the restriction if its width $h_{2,B}$ is less than $4k/V_L\rho c_p$. If the velocity of the cold gas outside the flame core, $U_{1,D}$ (downstream of the expansion) or $U_{1,C}$ (upstream of the expansion), decelerates so that $\frac{U_{1,D}}{U_{1,C}} \leqq \sqrt{\frac{1 - \rho_2}{\rho_1}}$, flow reversal will take place. This is in an assumed absence of lateral momentum transport, which inhibits flow reversal. As flow reversal is approached, the large velocity differences between the more retarded streamlines and the less retarded neighbors serve as a source of turbulence that encourages the lateral transport of momentum. It is to this near flow reversal and its altered turbulence that the increased turbulent flame speed in the region downstream of the restriction is ascribed.

SUMMARY OF RESULTS

Measurements of turbulent flame speeds were made in a duct in which blockage had been introduced. The investigation was not exhaustive, but certain definite conclusions can be drawn:

1. Blockage is more beneficial when introduced downstream of a flameholder than at the flameholder; that is, for equivalent pressure drops, heat-release rates downstream are about 4 times those at the flameholder.

2. The shape of the blockage influences the gains; symmetrical obstructions that restricted the flow for a finite distance were found to be the most effective.

3. When a flameholder is placed within or immediately upstream of a convergent section, the flame is prone to blow out; however, for a divergent section blowout does not occur.

CONCLUDING REMARKS

The extrapolation of the present work that most readily suggests itself is the afterburner application. In this case, small flameholders having the minimum width demanded by stability requirements followed by streamlined obstructions could offer advantages of low drag without burning and high space-heating rates with burning.

Lewis Flight Propulsion Laboratory
National Advisory Committee for Aeronautics
Cleveland, Ohio, August 19, 1957

APPENDIX A

SYMBOLS

A	area, sq ft
c_p	specific heat at constant pressure of combustion air, Btu/(lb)($^\circ$F)
d	quenching distance, in.
E	voltage
F	fraction burned
f	fuel-air ratio
g	gravitational constant, 32.2 ft/sec^2
h	flame width, ft
k	thermal conductivity
m	mass-flow rate, slugs/sec
P	total pressure
p	static pressure
Q	heat of combustion, Btu/lb
q	volumetric heat-release rate, (Btu/hr)/cu ft
T	static temperature, $^\circ$R
U	velocity in x-direction, ft/sec
V	flame speed, ft/sec
x	distance along horizontal centerline of combustor measured from combustor inlet
α	thermal diffusivity, k/c_p
ε	inlet kinetic energy
η	efficiency
ρ	density, slugs/cu ft

Subscripts:

B	plane of maximum convergence in restriction
C	plane of divergence in restriction
D	plane of exit in restriction
a	air
b	theoretical flame
c	combustion
F	flame
L	laminar
max	maximum
T	turbulent
0	approach flow
1	local cold gas
1D	theoretical one-dimensional flow
2	local hot gas

Superscript:

$\bar{}$	averaged over the hot gas

APPENDIX B

DERIVATION OF THE PRESSURE-DROP PARAMETER $\Delta P_{actual}/\Delta P_{1D}$

Assuming incompressible inviscid non-heat-conducting fluid throughout and neglecting gravity, the equations necessary for the one-dimensional case are

Momentum:

$$pA + mU = \text{constant} \tag{B1}$$

Bernoulli:

$$P = p + \tfrac{1}{2}\rho U^2 \tag{B2}$$

Continuity:

$$m = \rho AU = \text{constant} \tag{B3}$$

The total-pressure drop across the flame will be

$$P_1 - P_2 = p_1 - p_2 + \tfrac{1}{2}\rho_1 U_1^2 - \tfrac{1}{2}\rho_2 U_2^2 \tag{B4}$$

Substituting equation (B3) into (B1) gives, for A = constant,

$$0 = p_1 + \rho_1 U_1^2 - (p_2 + \rho_2 U_2^2) \tag{B5}$$

Subtracting equation (B5) from (B4), gives

$$P_1 - P_2 = \tfrac{1}{2}\rho_2 U_2^2 - \tfrac{1}{2}\rho_1 U_1^2 = \tfrac{1}{2}\rho_1 U_1^2 \left(\frac{U_2}{U_1} - 1\right) \tag{B6}$$

or, dividing by the inlet kinetic energy $\varepsilon = \tfrac{1}{2}\rho_1 U_1^2$,

$$\frac{P_1 - P_2}{\varepsilon} = \frac{U_2}{U_1} - 1 \tag{B7}$$

If changes in static pressure are neglected,

$$U_2 = U_1 \frac{T_2}{T_1} \tag{B8}$$

But

$$\frac{T_2}{T_1} = F\frac{T_b - T_1}{T_1} + 1 \tag{B9}$$

Therefore, substituting equations (B8) and (B9) into (B7) gives

$$\frac{P_1 - P_2}{\varepsilon} = F\left(\frac{T_b}{T_1} - 1\right) \tag{B10}$$

In the case of the stratified fluid, the flow is assumed to be (locally) parallel to the walls. The cold gas outside the flame zone has a flat velocity profile and a total pressure equal to that in the approach flow.

The hot gas inside the flame zone is assumed to have an arbitrary velocity (hence, total-pressure) profile, and its average total pressure will depend upon the history of the flow through the flame. At any station the static pressure is assumed constant. The gas that has passed through the flame is assumed completely burned. The local total pressure is

$$P = P_1(1 - F) + P_2F \tag{B11}$$

In the absence of lateral transport of energy, $P_0 = P_1$ so that total-pressure drop can be written

$$P_0 - P = F(P_1 - P_2) \tag{B12}$$

and, since the static pressure is constant for any cross section,

$$P_0 - P = F\left(\tfrac{1}{2}\rho_0 U_1^2 - \overline{\tfrac{1}{2}\rho_2 U_2^2}\right) \tag{B13}$$

where $\overline{\frac{1}{2}\rho_2 U_2^2}$ is averaged over the hot gas.

In rating the configurations tested it is desirable to put equation (B13) into these measurable quantities: $P_1 - p_1 = \frac{1}{2}\rho_0 U_1^2$ and F. To do this first divide equation (B13) by $\frac{1}{2}\rho_0 U_1^2$:

$$\frac{\Delta P}{\varepsilon} = F\left[\left(\frac{U_1}{U_0}\right)^2 - \frac{\rho_2}{\rho_1}\overline{\left(\frac{U_2}{U_0}\right)^2}\right] \tag{B14}$$

The term that was not measured is $\overline{(U_2/U_0)^2}$. As an approximation, take

$$\overline{(U_2/U_0)^2} = (\bar{U}_2/U_0)^2 \tag{B15}$$

then by definition

$$\frac{\rho_2 U_2}{\rho_0 U_0} = F \frac{A_0}{A_2} \tag{B16}$$

Similarly, where $A_1 + A_2 = A_0$ (where A_1 is area occupied by cold gas),

$$\frac{A_2}{A_0} = 1 - \frac{A_1}{A_0} = 1 - (1 - F) \frac{U_0}{U_1} \tag{B17}$$

Then with assumption (B15) and equations (B16) and (B17), equation (B14) becomes

$$\frac{\Delta P}{\varepsilon} = F \left\{ \left(\frac{U_1}{U_0} \right)^2 - \frac{\frac{\rho_0}{\rho_2} F^2}{\left[1 - (1 - F) \frac{U_0}{U_1} \right]^2} \right\} \tag{B18}$$

If again ρ_0/ρ_2 is taken to be T_b/T_0, then the pressure-drop parameter

$$\frac{\Delta P_{\text{eq.(B18)}}}{\Delta P_{\text{eq.(B10)}}} = \frac{\left(\frac{U_1}{U_0} \right)^2 - \frac{F^2 \left(\frac{T_b}{T_0} \right)}{\left[1 - (1 - F) \frac{U_0}{U_1} \right]^2}}{\frac{T_b}{T_0} - 1}$$

In the text this parameter is written $\Delta P/\Delta P_{1D}$.

APPENDIX C

ESTIMATION OF PARAMETERS CONTROLLING BURNER PERFORMANCE

A proper treatment of the flow through a restriction with accompanying chemical reaction and turbulent mixing would be a formidable task. In a similarly formidable problem, the case of a flame anchored in a straight constant-area duct, Scurlock (ref. 6) and Tsien (ref. 7) employed assumptions that remove the complexity introduced by the chemistry and the lateral transport and were able to predict certain aspects of the flow field that agree quite well with experiments. In this appendix similar simplyifying assumptions are made. The purposes of the appendix are to: (1) construct a qualitative picture of a flame in a duct flowing through a restriction; (2) estimate the parameters controlling flame extinction; and (3) estimate the geometrical influence of the downstream blockage on the performance with combustion.

Qualitative Picture of Flow Through a Restriction

When stratified layers of hot and cold gas are forced through a restriction, a number of things happen. If the hot and cold layers are separated by a flame front, as in the present case, this flame front becomes stretched. Then, because the same static-pressure gradient operates on all the gas, the hot gases are accelerated more rapidly than the cold and an exaggerated velocity profile results (see refs. 6 and 7). Then the gas that passes through the flame front within the restriction will have a lower total pressure than the gas that passed through upstream of the restriction, by virtue of its higher momentum pressure drop. A consequence of this latter occurrence is that the acceleration process cannot be reversed; the gas possessing inferior total pressure will (in the absence of a lateral transport of momentum) tend to reverse as the static pressure increases, and the flow will tend to separate within the hot gas. The following sketch illustrates these points:

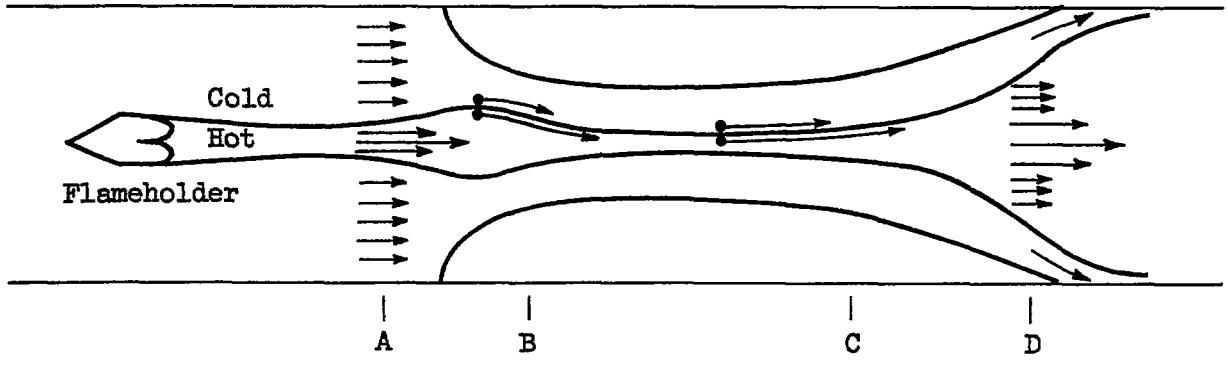

From the flameholder to station A the gas behaves nearly the way it would (refs. 6 and 7) if there were no obstruction present. If the acceleration from A to B is so rapid that negligible flame propagation occurs, there will be a velocity jump created at the flame front and the fluid elements that were marked in a circle at station A become separated as shown. This separation is an indication of the amount of stretching that a flame has undergone. In the plane case the amount of stretching, based on the velocity at the hot side of the flame, is obviously

$$\frac{dA_F}{A_F} = - \frac{dh_2}{h_2} \tag{C1}$$

Flame Extinction

There are two mechanisms proposed in the literature whereby stretching of the flame front could cause flame extinction. (1) If $h_{2,B}$ is of the order of a quenching distance, then the flame will be quenched. This is best illustrated in a calculation in Spalding (ref. 5, p. 187) originally made to demonstrate the extinction of isolated slabs of flame. (2) Karlovitz (ref. 8) has shown that stretching a flame surface in a velocity gradient reduces flame speed and presumably leads to flame extinction. A crude way of illustrating this effect in the present case is to propose some rate of heat release $Q[T]$ dependent only on the temperature within the flame. An example is given in the following plot:

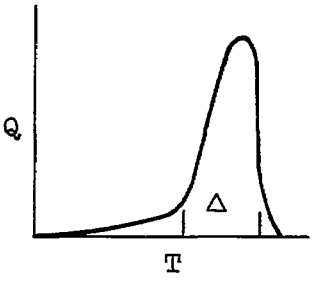

As the flame is rapidly stretched, the quantity of gas per unit area of flame front having a temperature within the range Δ, where most of the release occurs, is reduced; thus, either the flow of gas through the flame per unit area or the exit gas temperature or both must be reduced.

From figure 10 it can be noted that flame extinction occurs when the narrow flame just downstream of the recirculating zone is stretched by the restriction; when the flame is wider, that is, when the flameholder is moved farther upstream, the flame does not part. The rate of stretching in both cases should be nearly the same. Figure 11(e) illustrates a typical example of flame extinction caused by a stretching process. It

would appear, then, that extinction by the method of Karlovitz (ref. 8) does not apply here. On the other hand, when the flame parted, the flame zone was on the average about 0.10 inch wide. Because this zone is turbulent, it appears quite likely that the instantaneous value of flame-zone width is less than the quenching distance, which according to Spalding (ref. 5) is

$$h_{2,B} < d = 4\left(\frac{V_L\rho}{\alpha}\right)^{-1} = 4\left(\frac{V_L\rho c_p}{k}\right)^{-1} \approx 8.3\times10^{-4} \text{ ft} \qquad (C2)$$

Effect of Flame Spreading in Constriction

The velocity and total-pressure profiles at station B are sketched below.

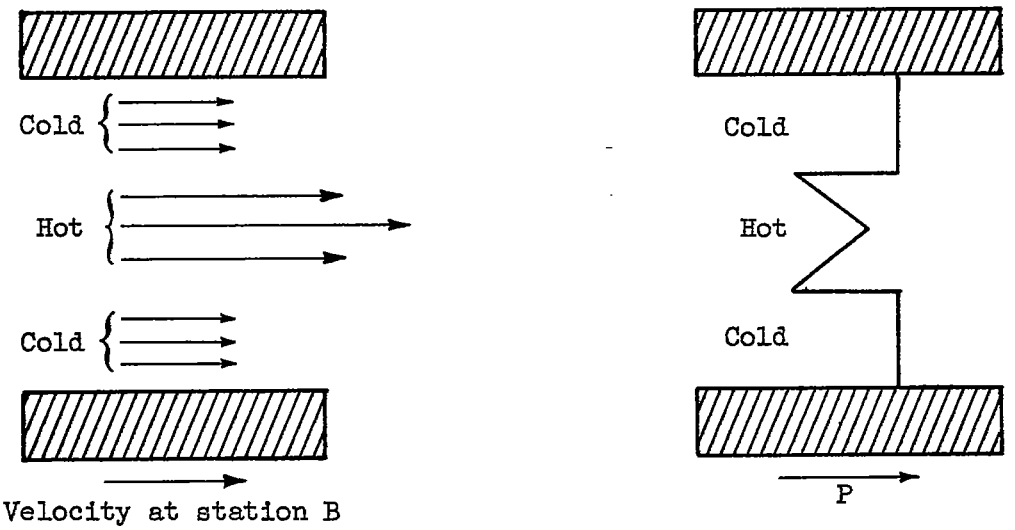

It can be shown that the total pressure for any stream tube is related to the static pressure and velocity at the place where the stream tube originally came through the flame:

$$P = p_F + \tfrac{1}{2}\rho_2 U_F^2 = P_0 - \tfrac{1}{2}\rho_1 U_F^2 + \tfrac{1}{2}\rho_2 U_F^2$$

or

$$P = P_0 - \frac{\rho_1 U_F^2}{2}\left(1 - \frac{\rho_2}{\rho_1}\right) \qquad (C3)$$

Then for the gas that passes through the flame within the throat restriction the total pressure will be lower according to equation (C3) than for the gas entering upstream. The resulting U and P profiles at station C are as follows:

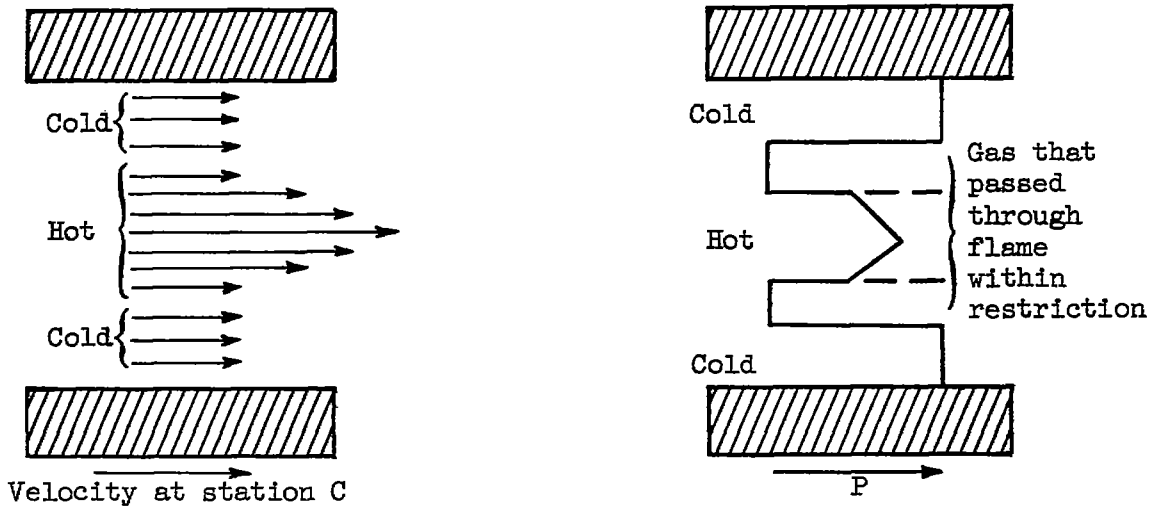

In order to bring the hot gas deficient in total pressure to rest, the pressure has to increase an amount

$$\Delta P = \frac{1}{2}\rho_2 U_{1,C}^2 \tag{C4}$$

or the ratio of cold-gas velocities needed to supply this pressure rise is

$$\frac{U_{1,D}}{U_{1,C}} = \sqrt{1 - \frac{\rho_2}{\rho_1}} \tag{C5}$$

In the tests on configuration A no flow separation either near the wall or within the flame could be detected. On the other hand, violent mixing and rapid combustion took place in the divergent section. This suggests that as the profile tends toward one in which flow reversal can occur it becomes unstable; transition to violent local turbulence occurs, and the lateral transport of momentum is sufficiently rapid to prevent separation. From station C to D the qualitative picture would appear to depend primarily on a balance between a pressure-gradient effect and the lateral transport of momentum. The following paragraph describes qualitatively this interaction.

Somewhere between the hot- and cold-gas interface and the centerline the total-pressure profile will go through a minimum. After a small amount of deceleration, the velocity profile will go through a minimum. This zone, then, will mix so that the velocity defect decays. If the pressure gradient is sufficient to overcome the rate of decay of the velocity defect, then flow reversal should occur. If, on the other hand, the profile is sufficiently unstable that violent mixing rapidly erases the velocity defect, no flow reversal will occur.

At present it appears that the latter more nearly fits the experimental results. Qualitatively, this flow instability would depend upon the magnitude of the total-pressure defect and the amount of gas affected. These in turn would depend upon the area blockage of the restriction and the amount of gas entering the flame in the restriction.

The configurations A to F (see table I) indicate that increased blockage increased the instability. The results of the series A, G, H, and I, in which blockage remained constant and length of restriction varied, indicate that the quantity of gas passing through the flame in the restriction has a more complicated relation.

REFERENCES

1. Blackshear, Perry L., Jr.: Growth of Disturbances in a Flame-Generated Shear Region. NACA TN 3830, 1956.

2. Clark, Thomas P., and Bittker, David A.: A Study of the Radiation from Laminar and Turbulent Open Propane-Air Flames as a Function of Flame Area, Equivalence Ratio, and Fuel Flow Rate. NACA RM E54F29, 1954.

3. Dugger, Gordon L.: Effect of Initial Mixture Temperature on Flame Speed of Methane-Air, Propane-Air, and Ethylene-Air Mixtures. NACA Rep. 1061, 1952. (Supersedes NACA TN's 2374 and 2170.)

4. Longwell, John P., and Weiss, Malcolm, A.: High Temperature Reaction Rates in Hydrocarbon Combustion. Ind. and Eng. Chem., vol. 47, no. 8, Aug. 1955, pp. 1634 to 1643.

5. Spalding, D. B.: Some Fundamentals of Combustion. Academic Press, Inc., 1955.

6. Scurlock, A. C.: Flame Stabilization and Propagation in High-Velocity Gas Streams. Meteor Rep. 19, Fuels Res. Lab., M.I.T., May 1948. (Contract NOrd 9661.)

7. Tsien, H. S.: Influence of Flame Front on the Flow Field. Jour. Appl. Mech., vol. 18, no. 2, June 1951, pp. 188-194.

8. Karlovitz, B., Denniston, D. W., Jr., Knapschaefer, D. H., and Wells, F. E.: Studies on Turbulent Flames. A. Flame Propagation Across Velocity Gradients. Fourth Symposium (International) on Combustion, The Williams & Wilkins Co. (Baltimore), 1953, pp. 613-617.

TABLE I. - SUMMARY OF CONFIGURATIONS AND RESULTS

[Free-stream velocity, 50 ft/sec; fuel-air ratio, 0.0456; laminar flame speed, 0.81 ft/sec.]

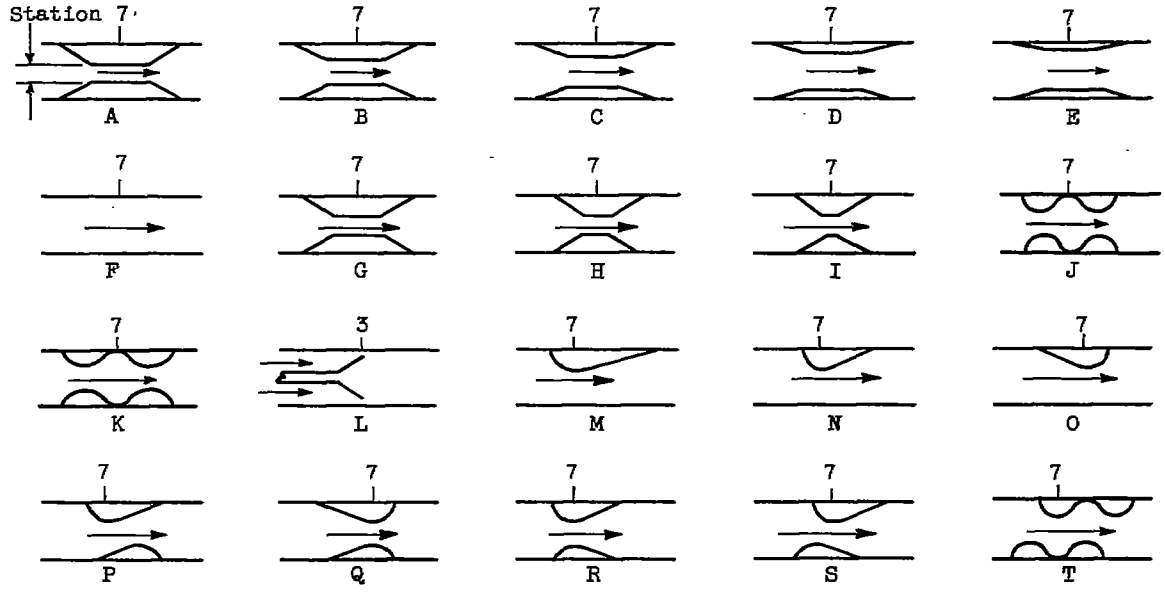

Configuration	Flame width, h, in.	Maximum turbulent flame speed, $V_{T,max}$	Combustion efficiency, η_c	Experimental pressure-drop parameter, $\Delta P/\varepsilon$	Theoretical one-dimensional pressure-drop parameter, $\Delta P/\Delta P_{1D}$
A	0.75	[a]5.50	[a]42.1	3.73	1.72
B	1.00	[a]5.02	[a]34.9	2.84	1.58
C	1.25	3.48	31.9	2.17	1.32
D	1.50	[a]2.35	[a]25.7	1.16	.874
E	1.75	1.70	21.9	.886	.785
F	2.00	[a]1.30	[a]18.1	.619	.665
G	.75	[a]4.05	[a]27.1	2.66	1.91
H	.75	3.40	29.0	2.75	1.84
I	.75	3.40	[a]33.7	2.22	1.54
J	.75	[a]4.45	[a]34.6	3.43	2.66
K	1.25	[a]3.64	[a]27.3	1.58	1.12
L	1.50	1.33	18.0	.72	.776
L	1.25	1.42	17.9	.878	.95
L	1.00	1.42	17.75	1.12	1.23
L	.75	1.42	17.65	1.50	1.65
L	.50	1.35	14.7	1.57	2.05
M	1.25	[a]2.54	[a]26.8	1.33	1.02
N	1.25	2.35	[a]25.8	1.22	1.02
O	1.25	2.67	28.6	1.64	1.11
P	.75	3.89	[a]34.5	1.91	1.30
Q	.75	3.81	32.7	3.40	2.02
R	.75	3.97	[a]39.2	2.01	1.18
S	.75	3.16	30.3	2.46	1.58
T	.75	4.05	33.7	3.30	1.90

[a]Obtained by extrapolation.

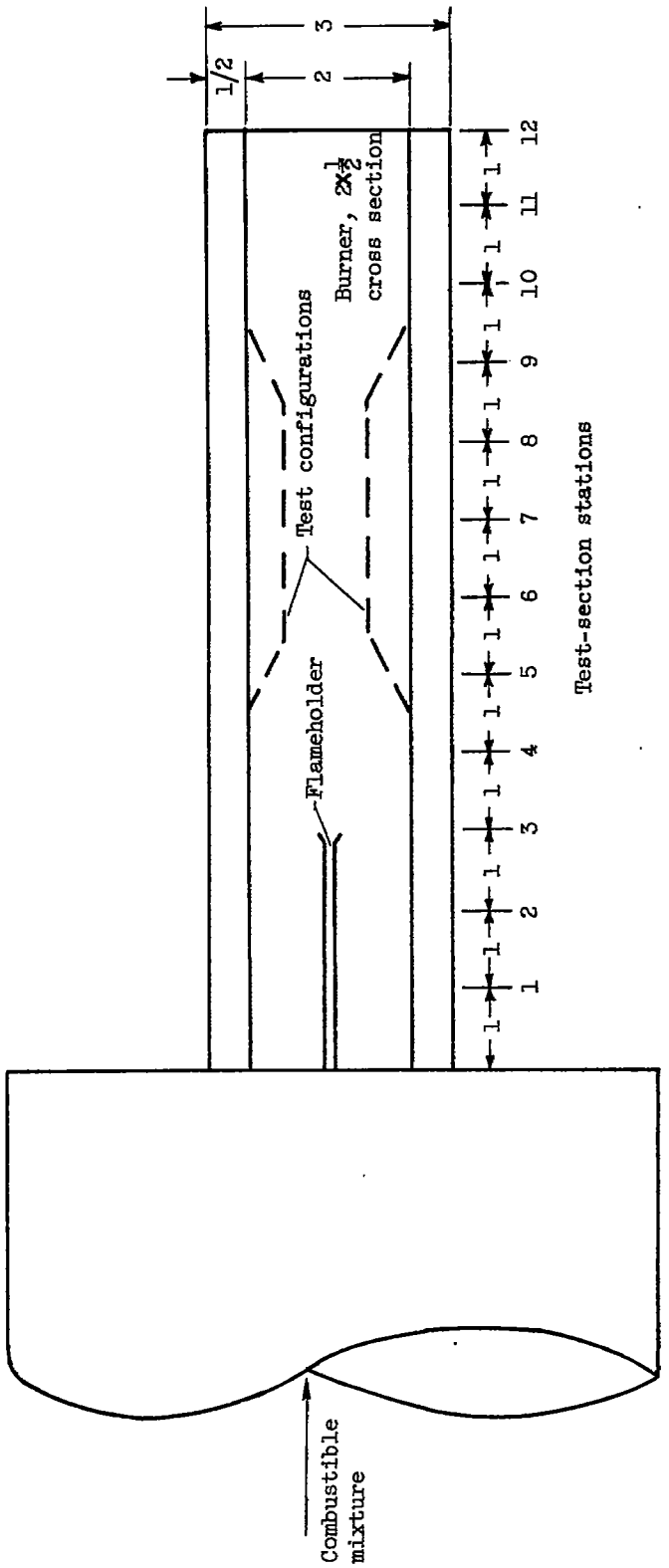

Figure 1. - Test section. (All dimensions in inches.)

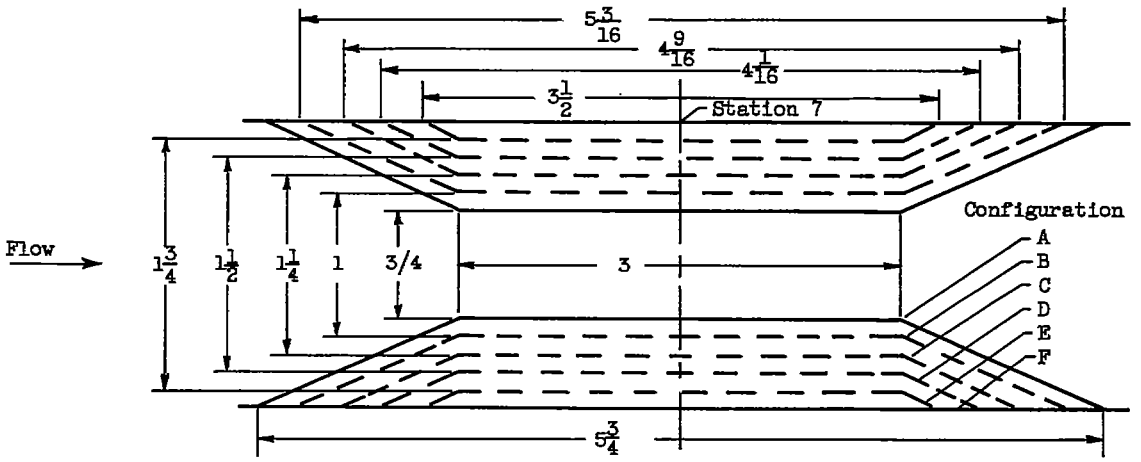

(a) Symmetric configurations. Burner cross-sectional blockages, 0 to $62\frac{1}{2}$ percent; constant throat length.

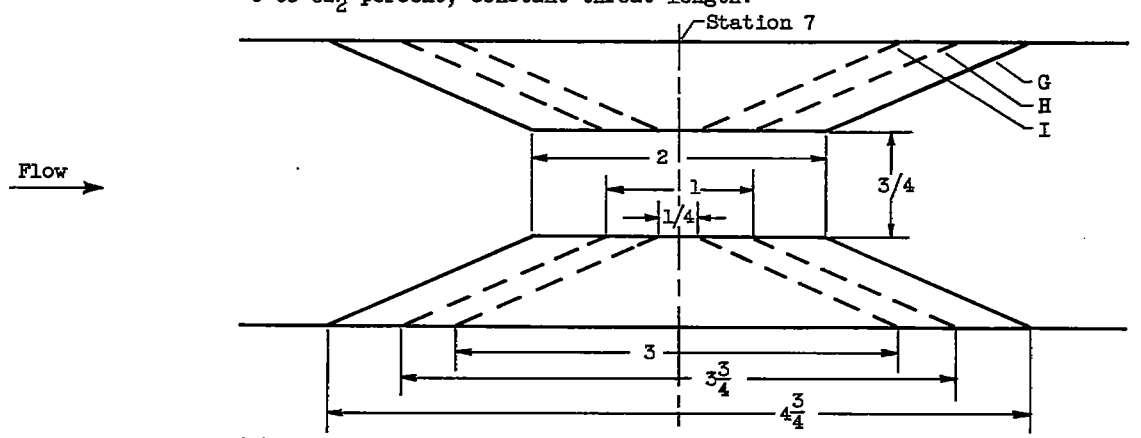

(b) Symmetric configurations. Burner cross-sectional blockage, $62\frac{1}{2}$ percent; variable throat length.

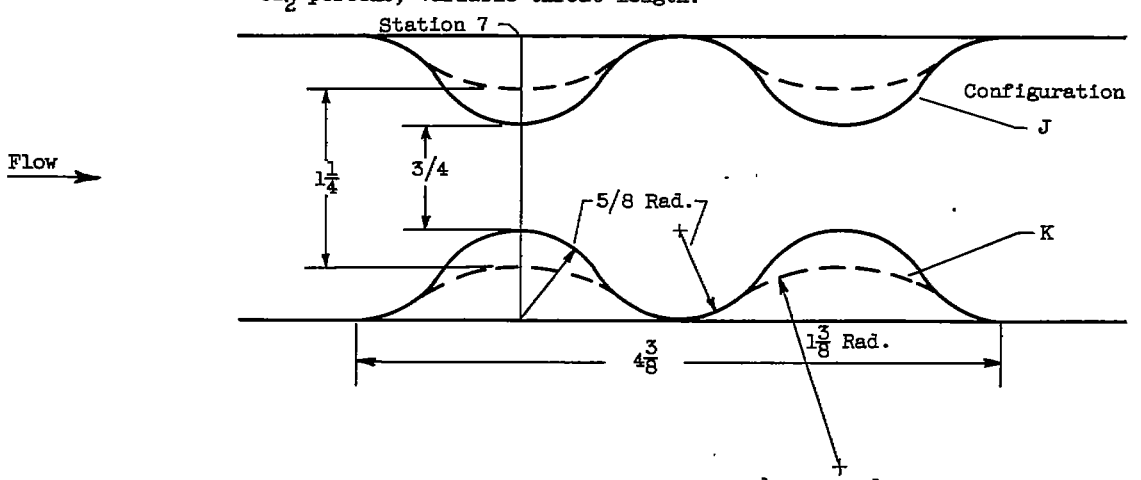

(c) Symmetric configurations J and K with $62\frac{1}{2}$ and $37\frac{1}{2}$ percent blockages, respectively.

Figure 2. - Test configurations. (All dimensions in inches.)

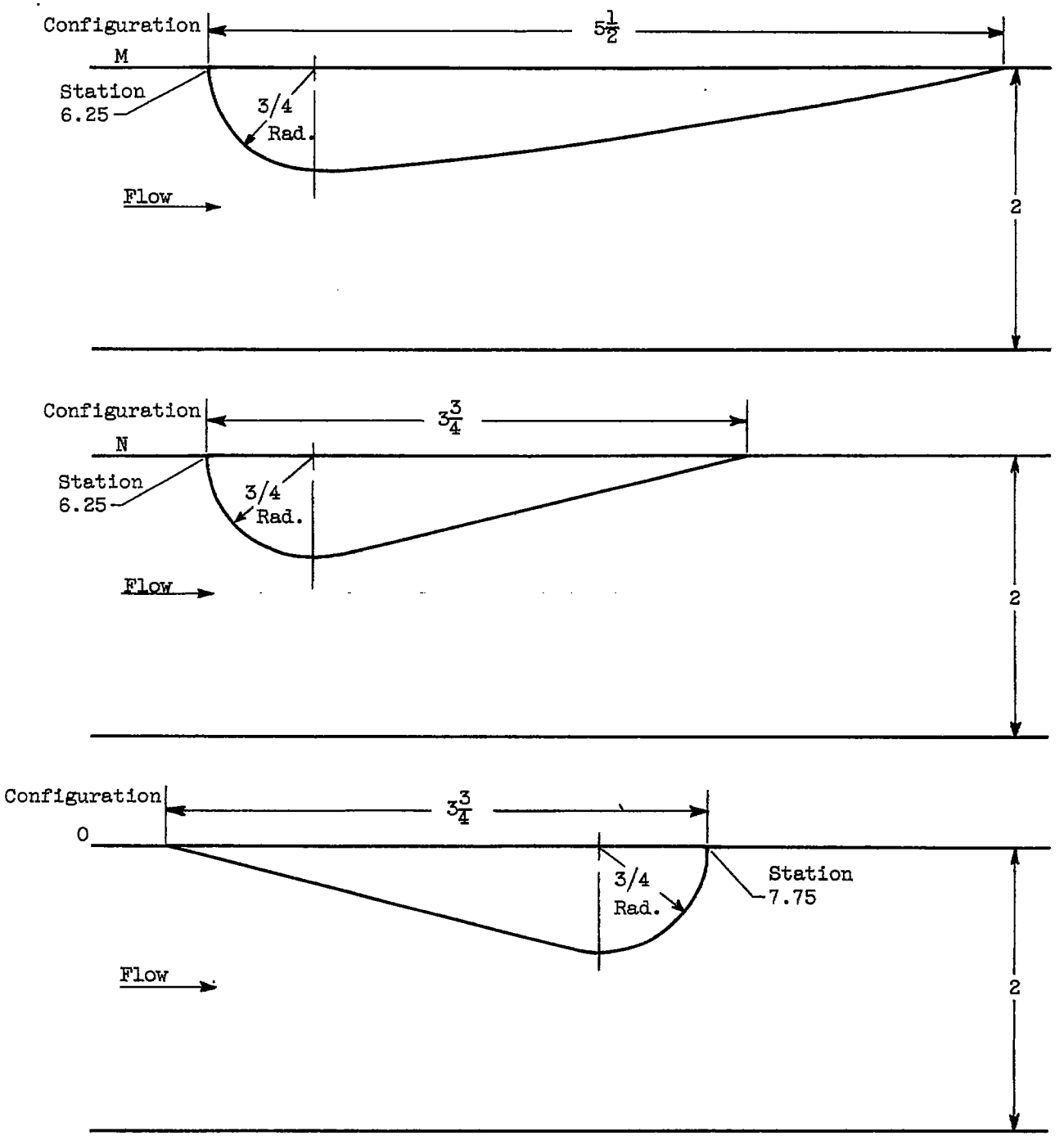

(d) Asymmetric configurations. Burner cross-sectional blockage, 37½ percent.

Figure 2. - Continued. Test configurations. (All dimensions in inches.)

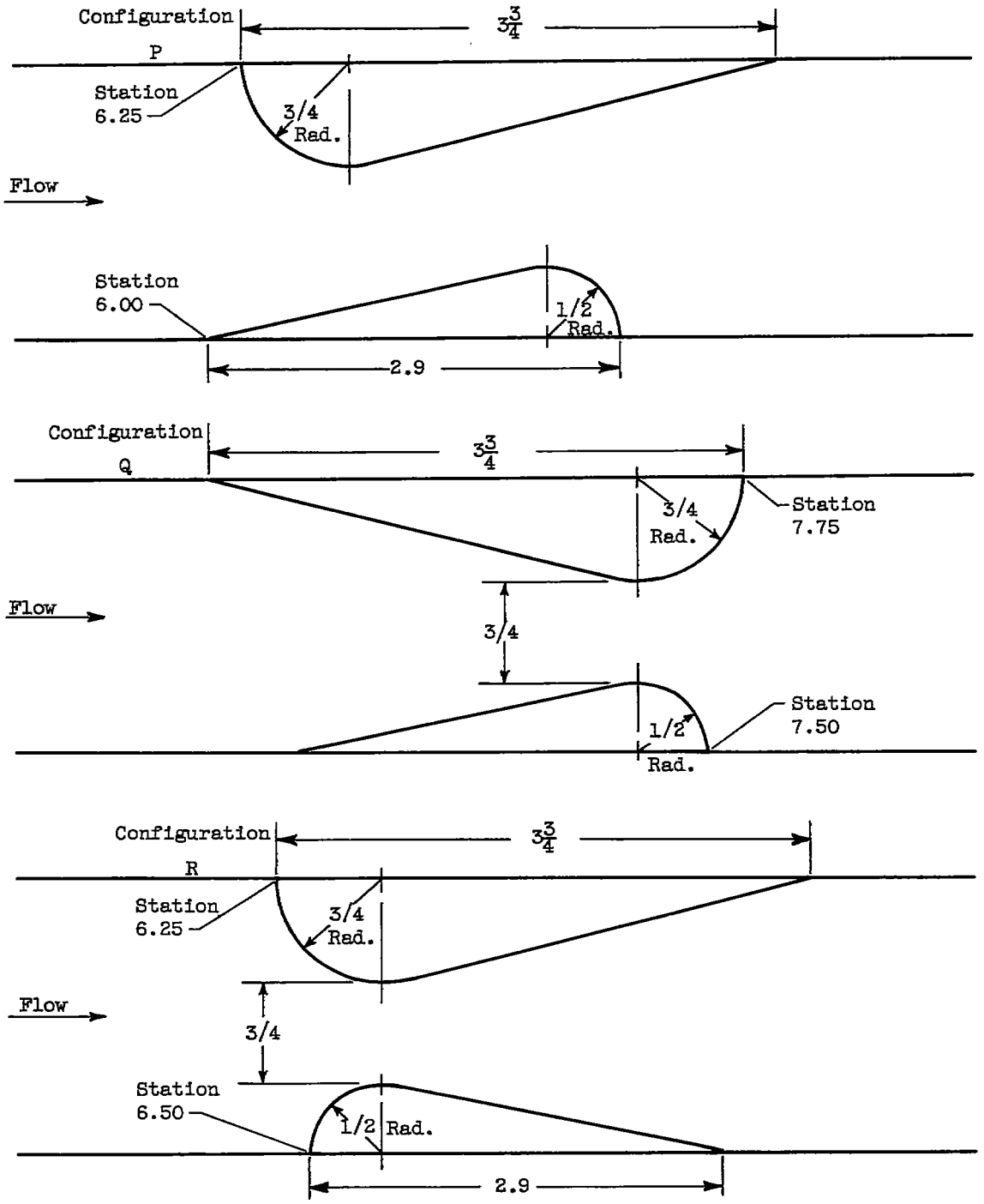

(e) Asymmetric configurations. Burner cross-sectional blockage, $62\frac{1}{2}$ percent.

Figure 2. - Continued. Test configurations. (All dimensions in inches.)

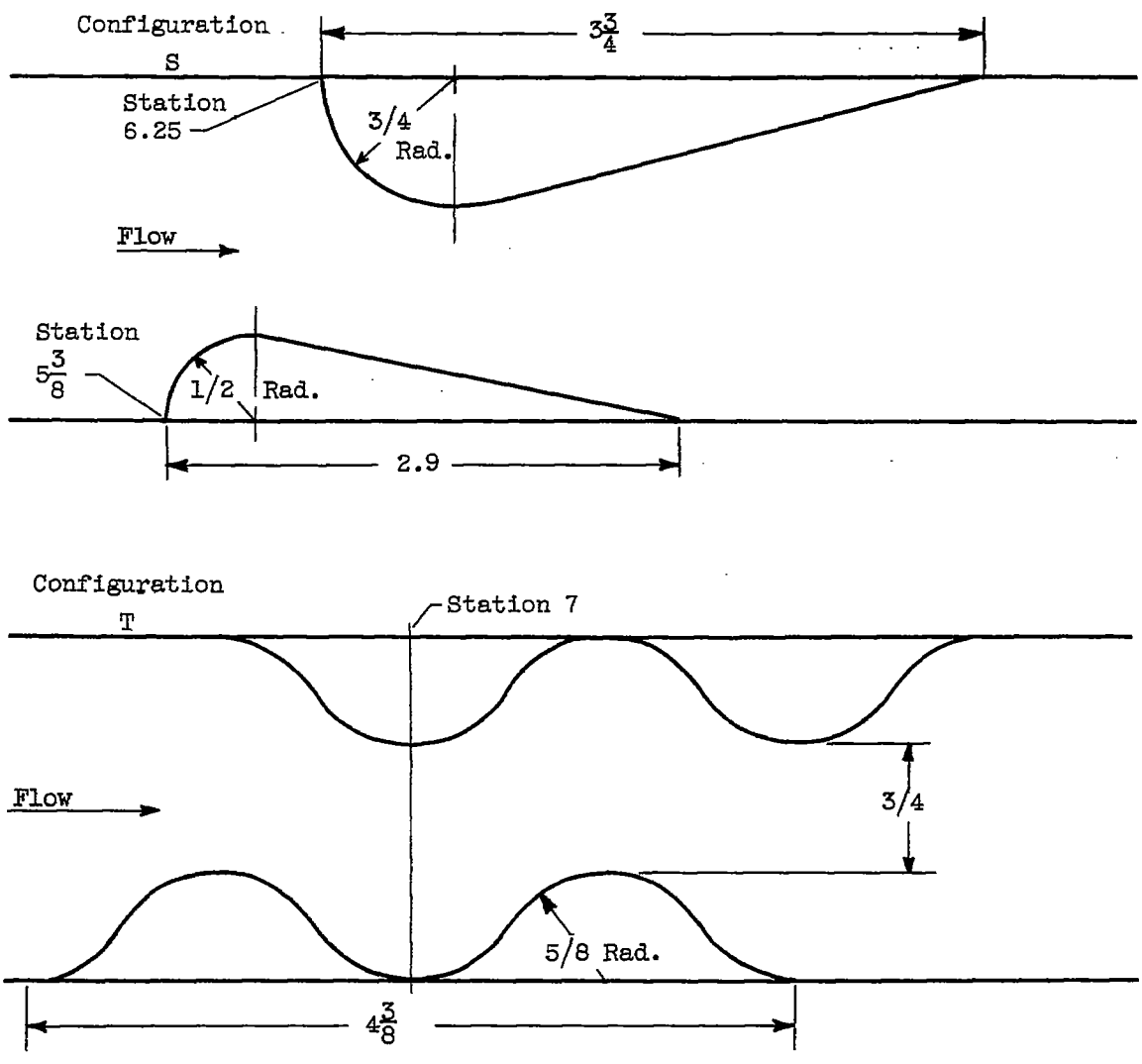

(e) Concluded. Asymmetric configurations. Burner cross-sectional blockage, $62\frac{1}{2}$ percent.

Figure 2. - Concluded. Test configurations. (All dimensions in inches.)

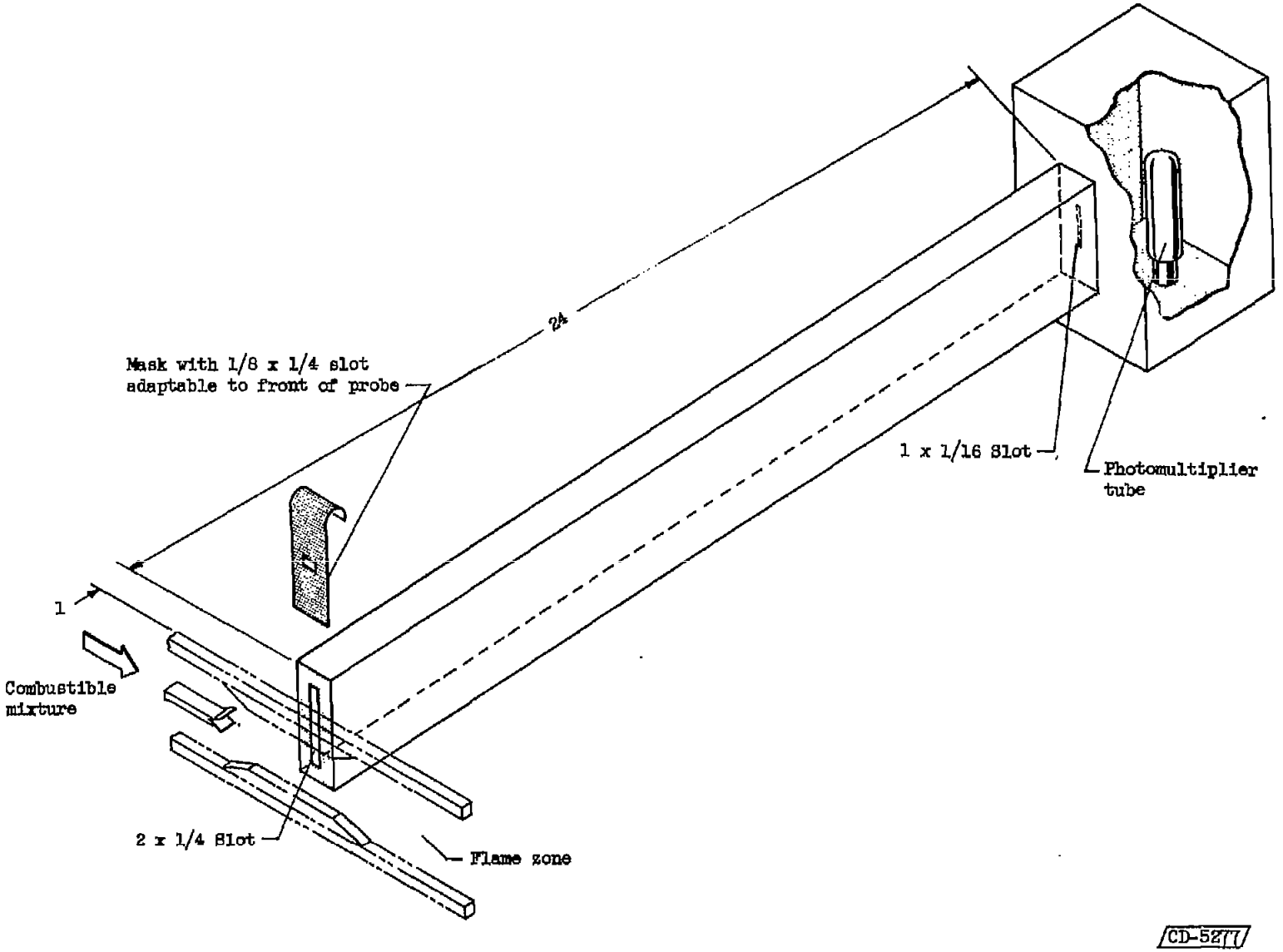

Figure 3. - Sketch of photomultiplier probe showing arrangement of slots and mask and orientation with respect to flame zone. (All dimensions in inches.)

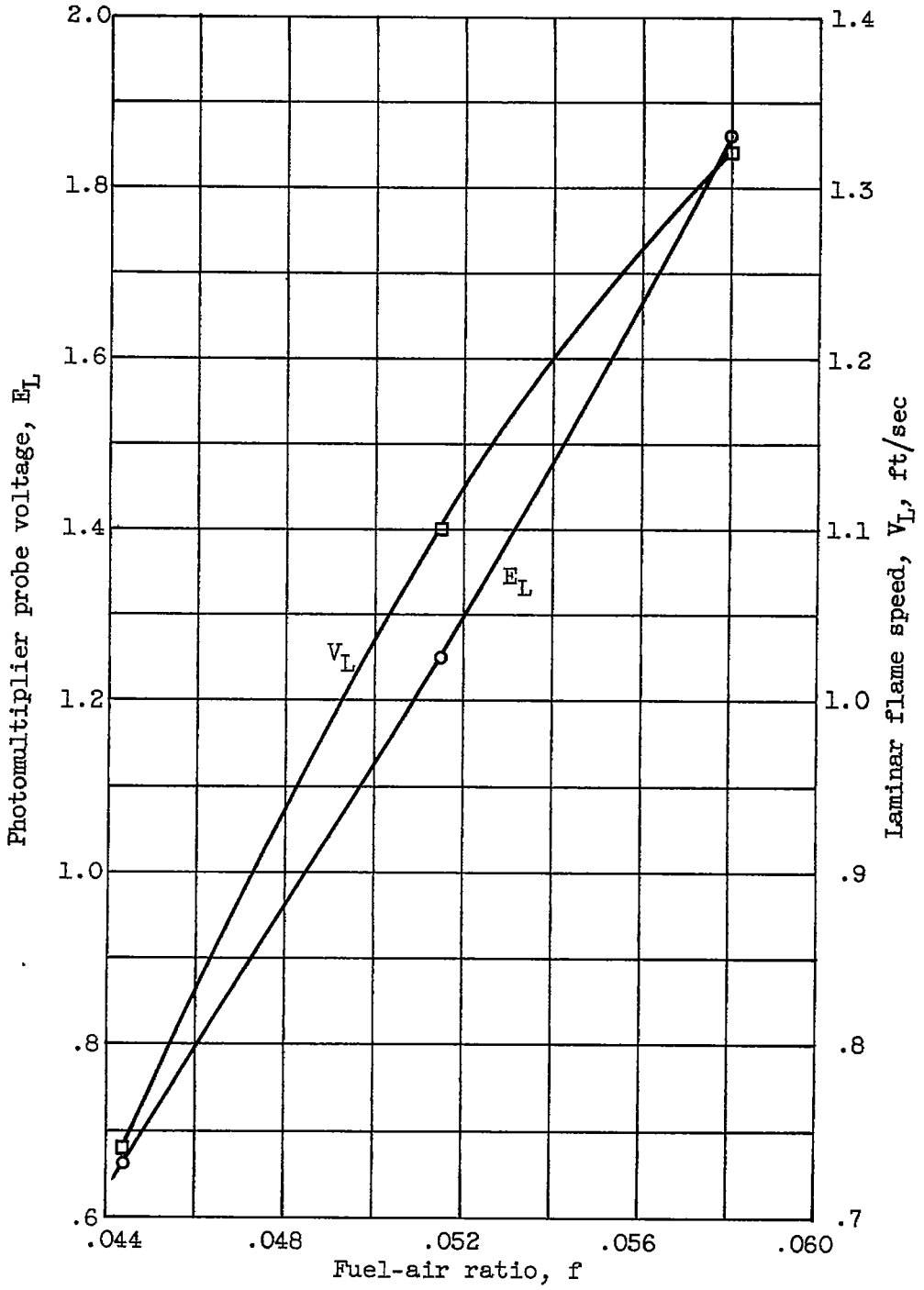

Figure 4. - Variation of laminar flame speed and photomultiplier probe voltage with fuel-air ratio. Values taken from reference 3.

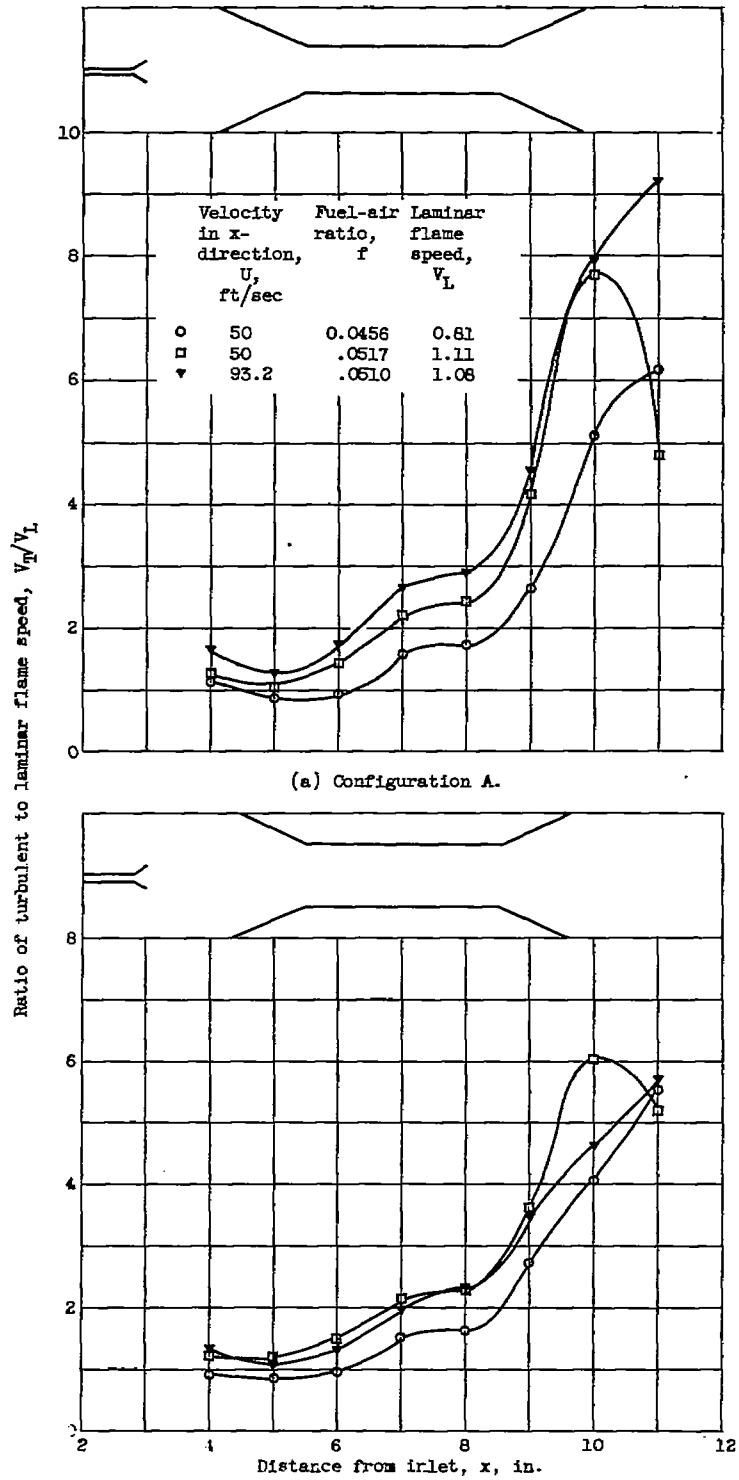

(a) Configuration A.

(b) Configuration B.

Figure 5. - Ratio of turbulent to laminar flame speed against distance from inlet for configurations A to F. Flameholder is at station 3.

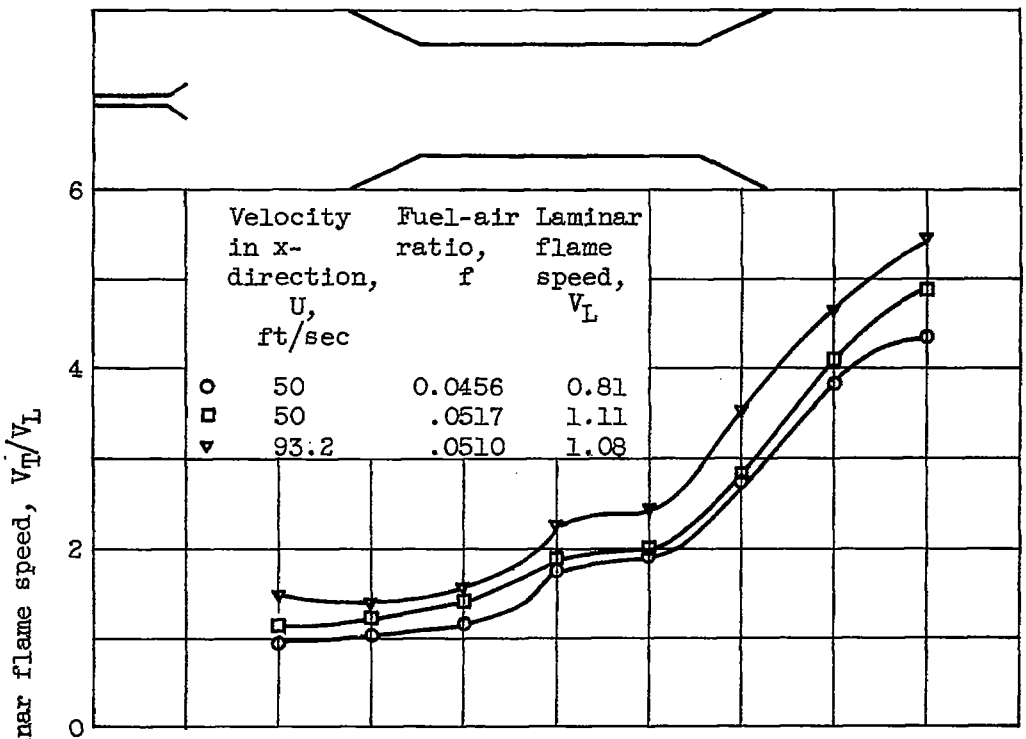

(c) Configuration C.

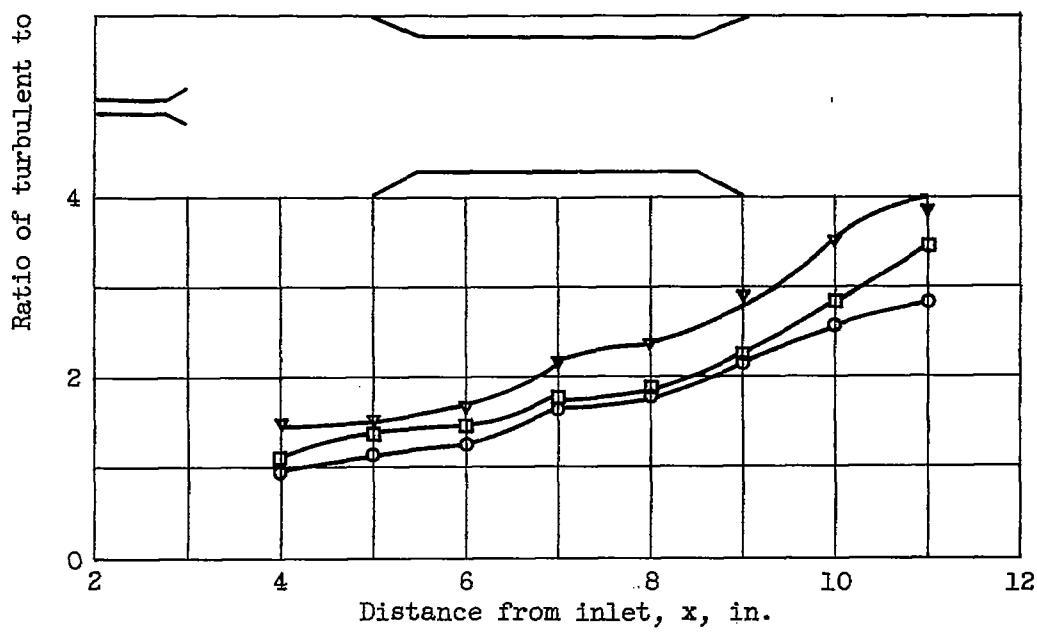

(d) Configuration D.

Figure 5. - Continued. Ratio of turbulent to laminar flame speed against distance from inlet for configurations A to F. Flameholder is at station 3.

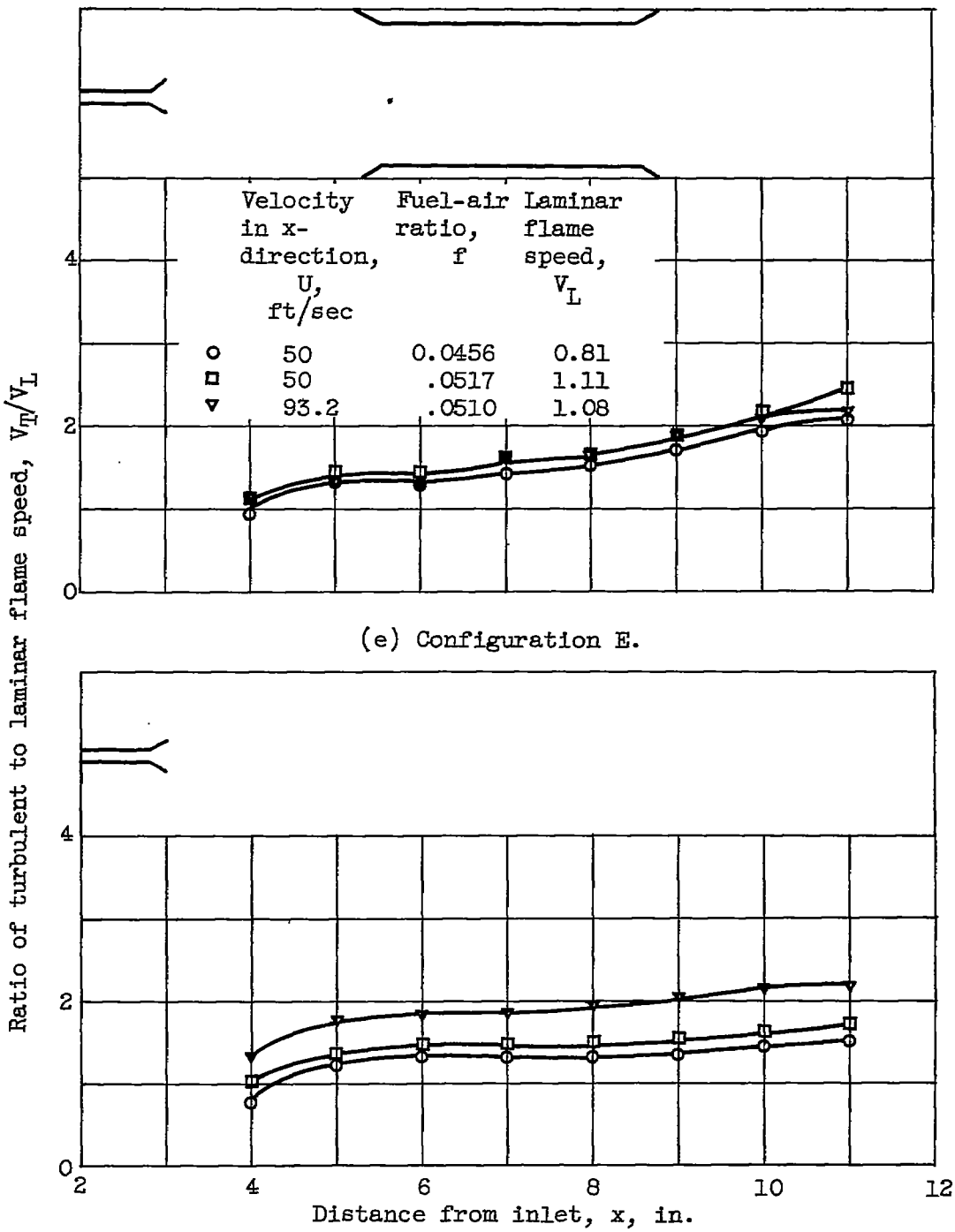

(e) Configuration E.

(f) Configuration F.

Figure 5. - Concluded. Ratio of turbulent to laminar flame speed against distance from inlet for configurations A to F. Flameholder is at station 3.

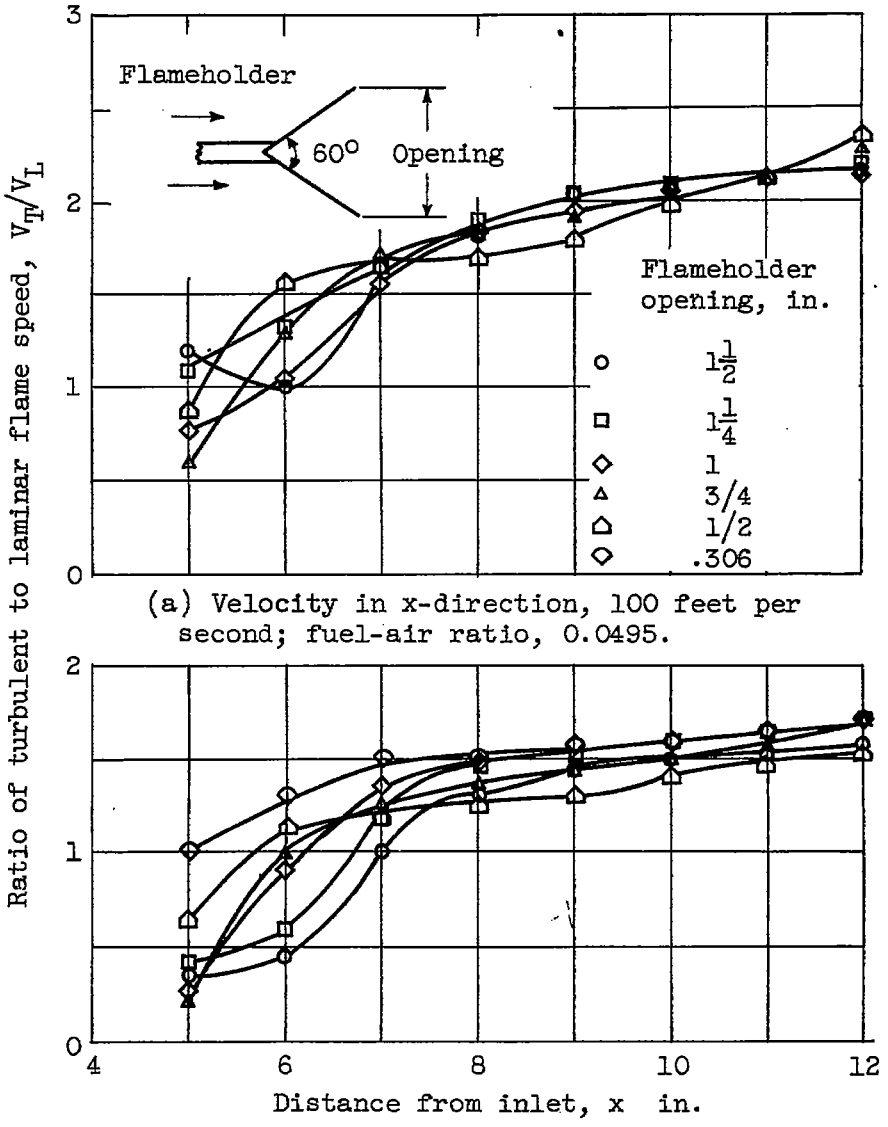

(a) Velocity in x-direction, 100 feet per second; fuel-air ratio, 0.0495.

(b) Velocity in x-direction, 50 feet per second; fuel-air ratio, 0.0467.

Figure 6. - Effect of flameholder size on ratio of turbulent to laminar flame speed. Flameholder is at station 4.

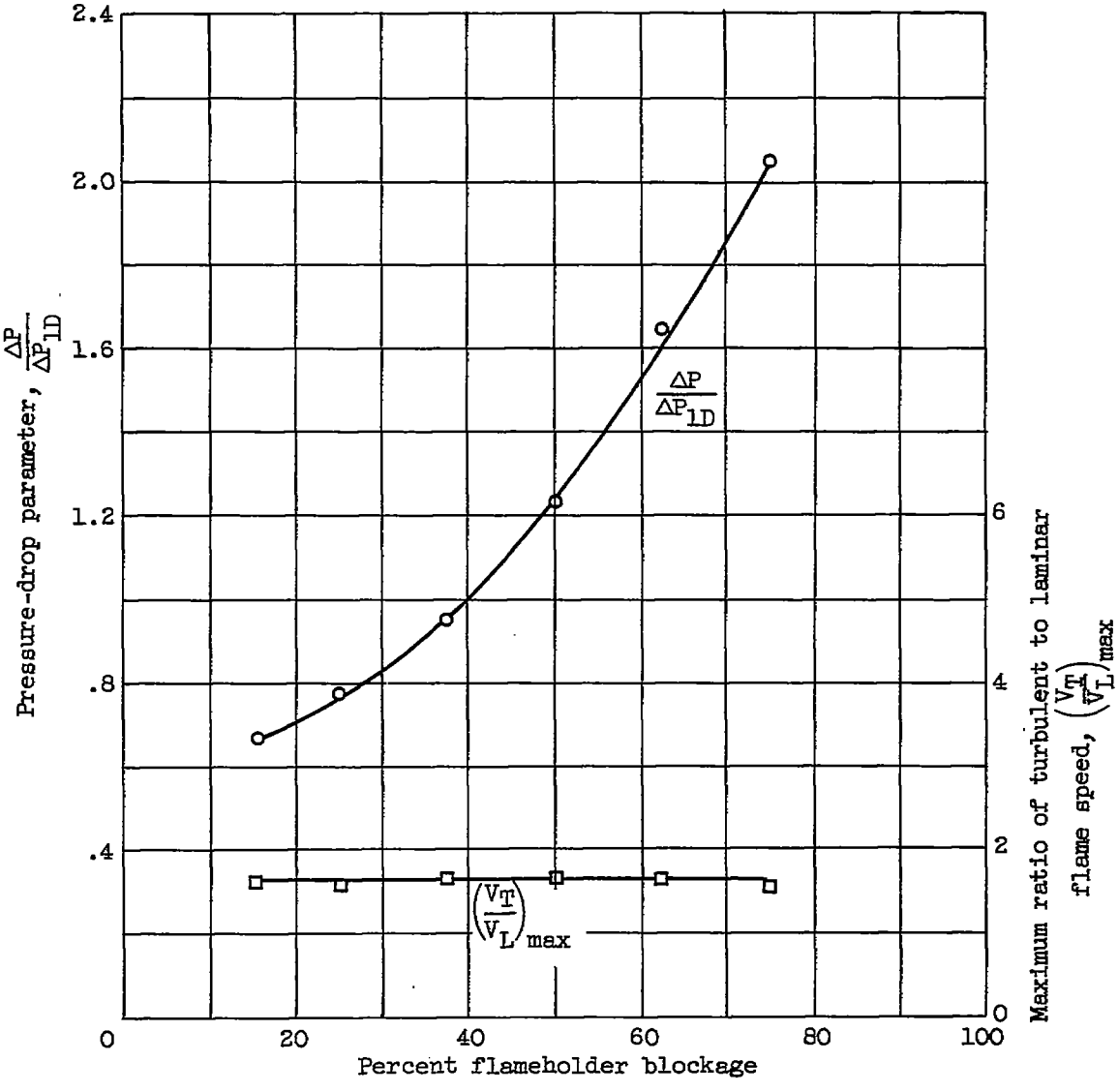

Figure 7. - Effect of flameholder blockage on pressure-drop parameter and maximum ratios of turbulent to laminar flame speeds. Velocity in x-direction, 50 feet per second; fuel-air ratio, 0.0467; flameholder at station 4.

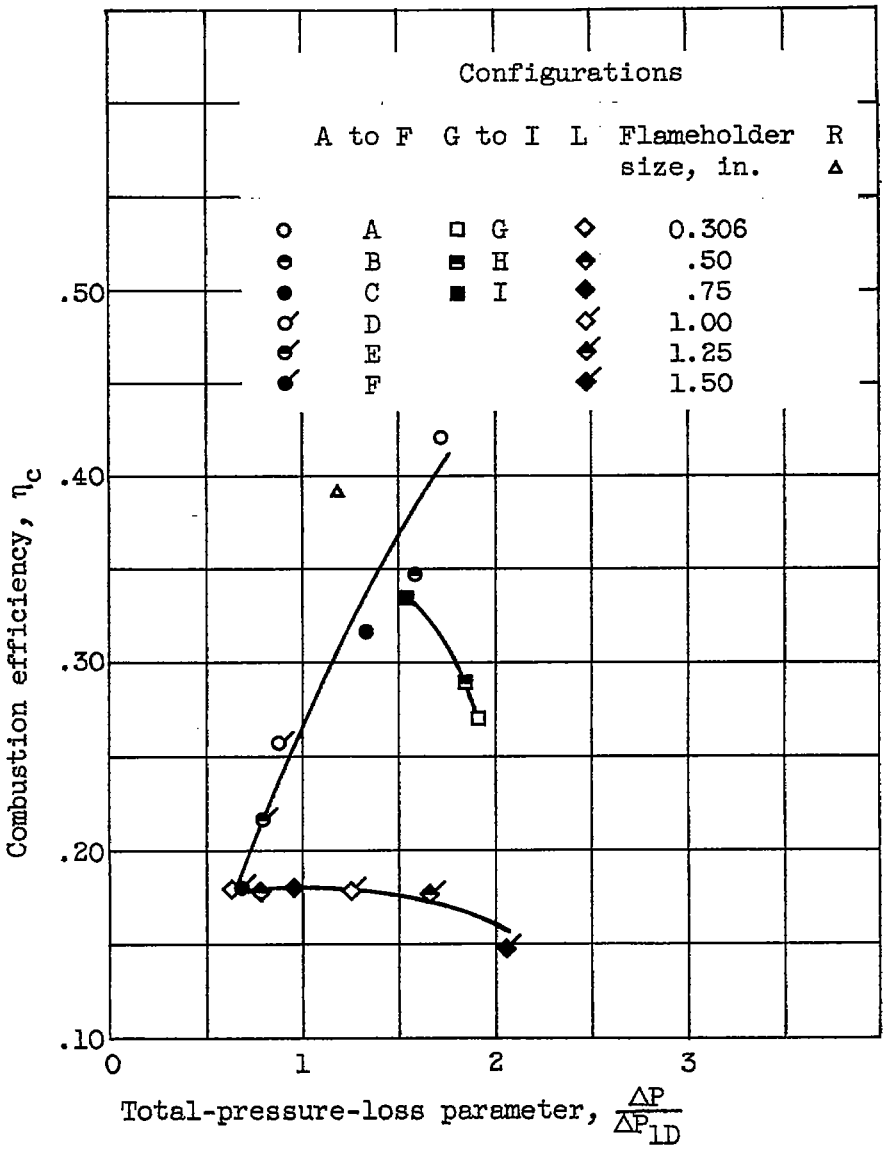

Figure 8. - Variation of combustion efficiency with total-pressure-loss parameter for four series of configurations.

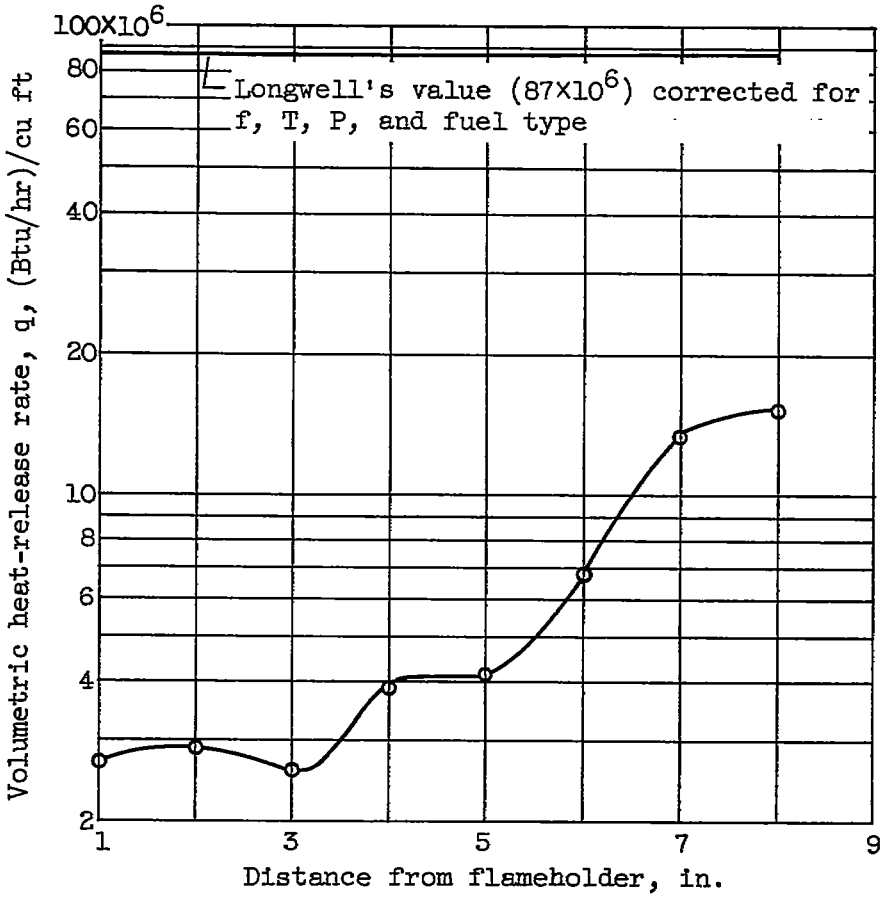

(a) Longitudinal measurement of volume heating rate.

Figure 9. - Volume heating rates for configuration A.

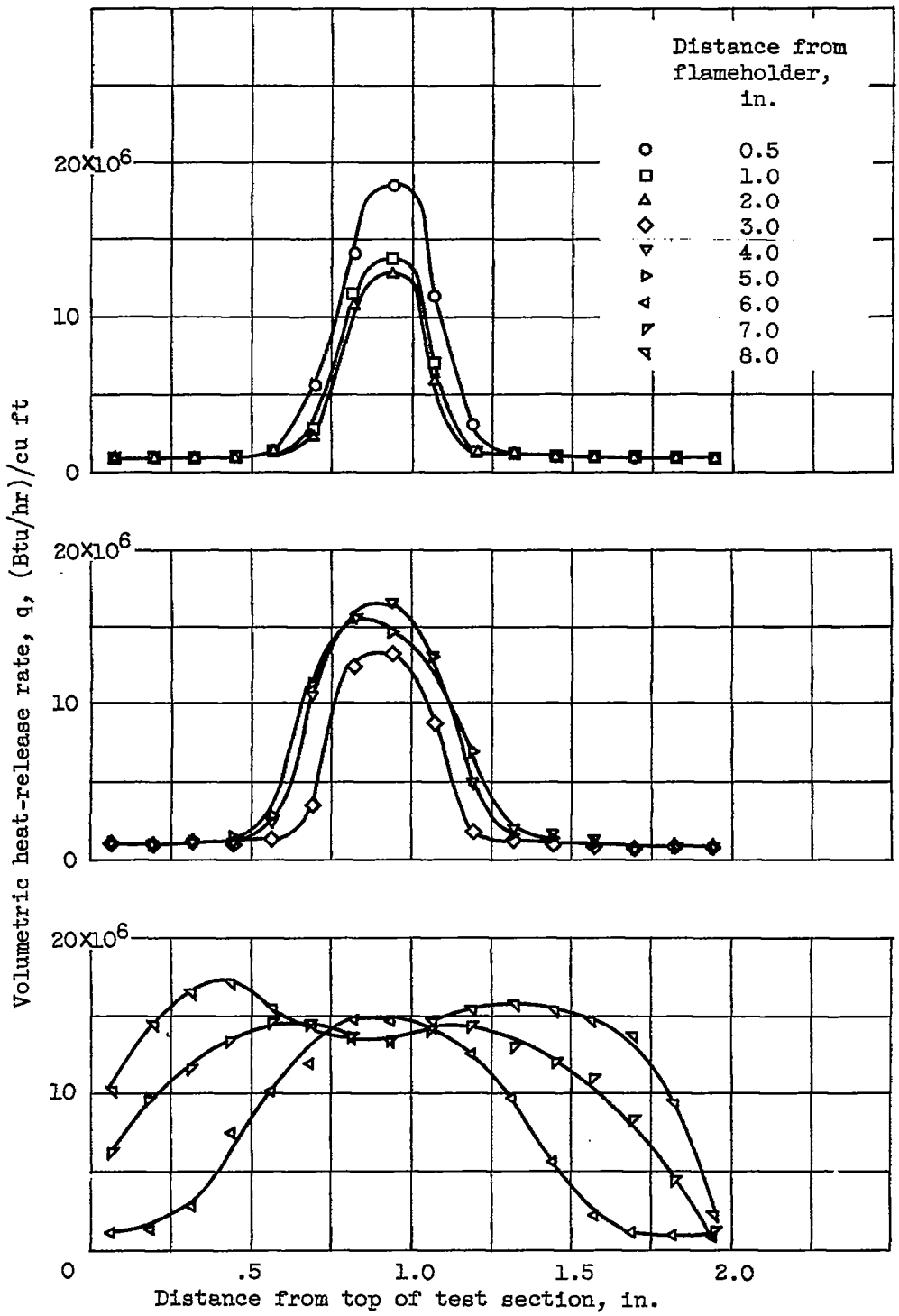

(b) Transverse measurements of volumetric heating rates.

Figure 9. - Concluded. Volume heating rates for configuration A.

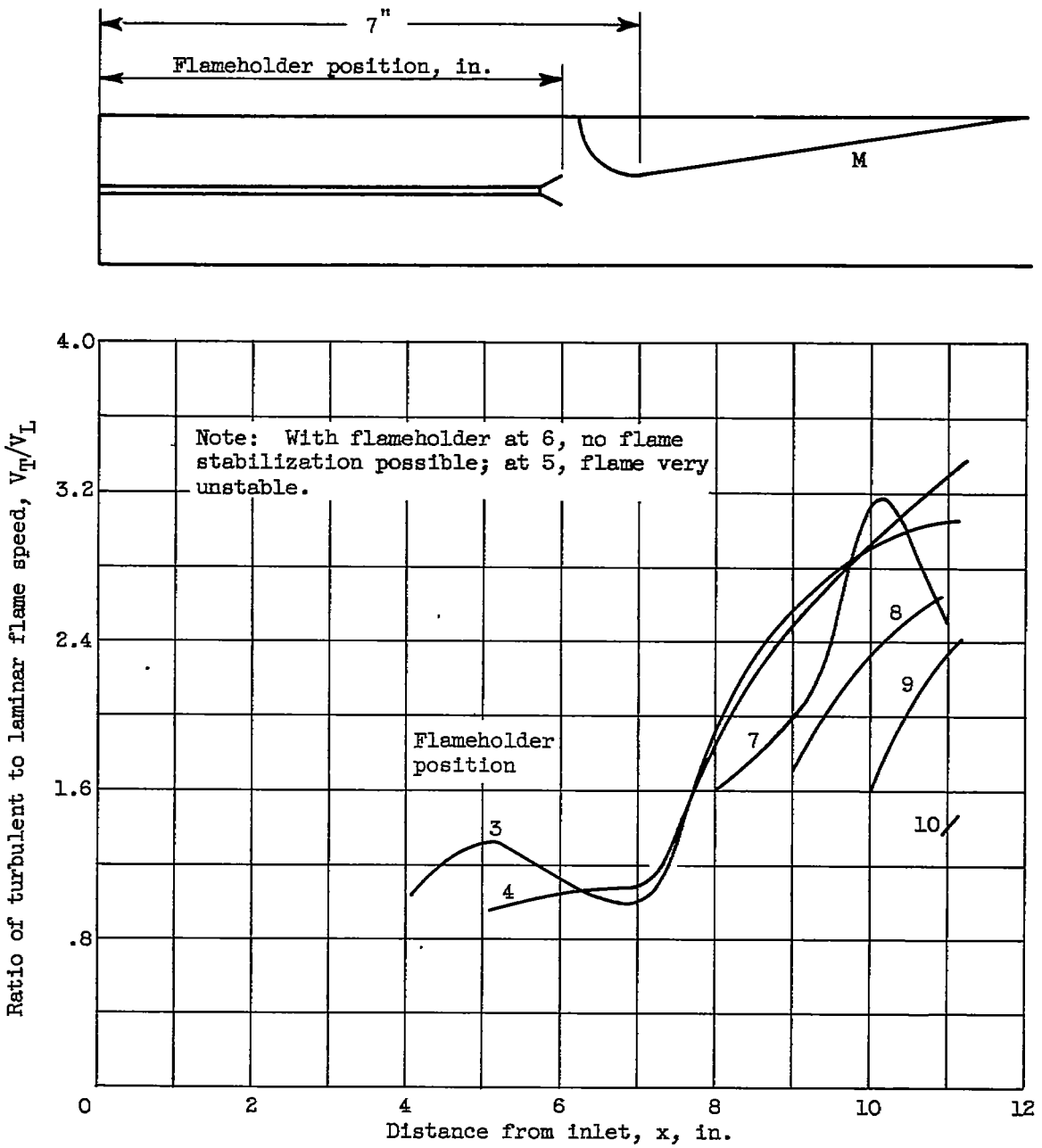

Figure 10. - Effect of flameholder and blockage positions on flame stability for configuration M.

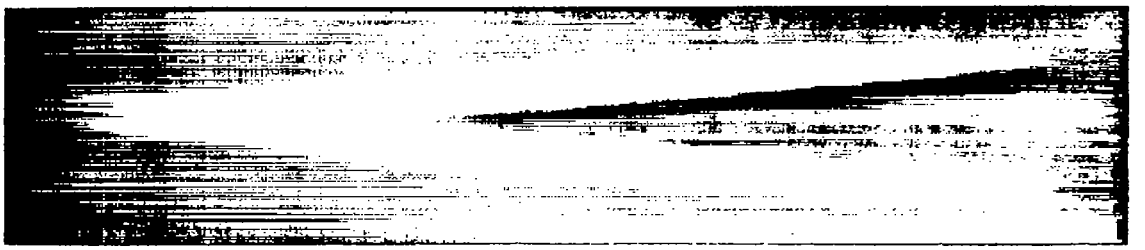

(a) Direct photograph of flame without additional blockage.

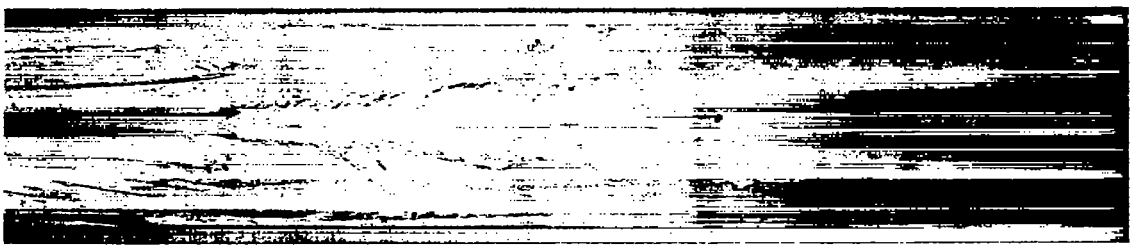

(b) Shadowgraph of flame without additional blockage.

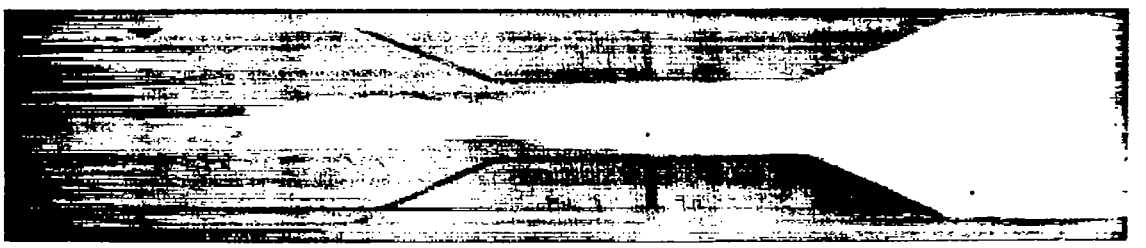

(c) Direct photograph of flame with configuration A.

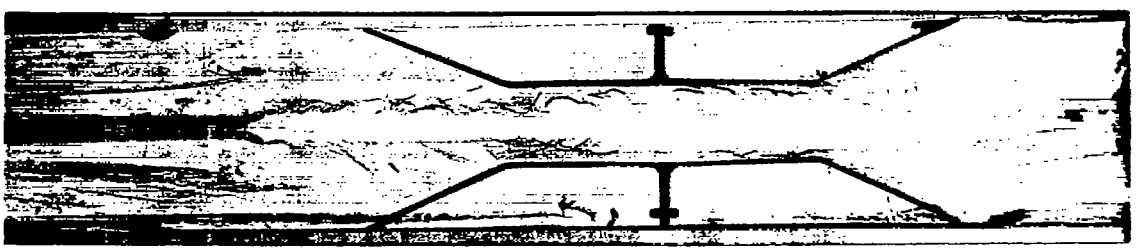

(d) Shadowgraph of flame with configuration A.

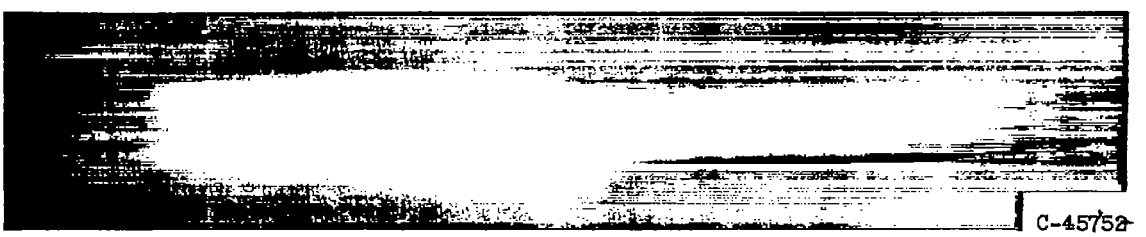

(e) Direct photograph of flame showing flame extinction at the contraction, configuration A.

Figure 11. - Flame photographs.